

## A Study on Fire Characteristics in a Tall and Narrow Atrium

by

Osami Sugawa\*, Wataru Takahashi\*\*, Masanori Ohtake\*\*\* and Hiroomi Satoh\*\*\*\*

\*Center for Fire Science and Technology, Science University of Tokyo

\*\* Dai-Nippon Construction, Research and Development Section

\*\*\* Kajima Corporation (Graduate Student of Science University of Tokyo)

\*\*\*\*Kajima Research Institute, Kajima Corporation

### ABSTRACT

The modeling on fire safety assessment for a tall and narrow atrium is carried out using a reduced and full scale atrium models based on the performances of flow behavior in and near corner fire and smoke ventilation system. The corner (or wall) effects on the flame behavior considering air entrainment into a flame was evaluated theoretically and experimentally. Temperature, upward velocity, inlet air velocity, and pressure difference between the atrium space and atmosphere were measured systematically in a reduced scale model. The performance of the modeling to estimate temperature rise and natural air ventilation volume was verified based on the experimental results. Smoke filling rate from a model fire source set at the center of a tall and narrow atrium is fastest in the other cases in which fire source set in or near a corner. This suggested that the centering of the fire source is acceptable as the fire source position to assess the fire safety design for a tall and narrow atrium.

### 1. Introduction

Atrium space is classified roughly into three groups, i.e., gallery or arcade type, cube type, and tall-and-narrow type. ASHRAE prepared the fire safety evaluation procedure for the first two types [1] but not for the last. Satoh et al. [2,3] reported the simplified estimation model on excess temperature and on the inlet air volume for a tall and narrow atrium based on the experimental and theoretical study using full scale models and a reduced scale model. Their model is established based on the natural ventilation performances induced by a fire. They also pointed out the influence of induced inlet air into the flame, but little is known on its behavior. In this paper, in order to obtain the quantitative understanding on the air entrainment into a flame/plume region, a fire source was set in and near corner and at the center of the atrium. Temperature and upward velocity in a reduced scale mode of tall and narrow atrium was measured systematically changing the inlet openings area and heat release rate. The first test series was carried out to evaluate the flow characteristics in and near corner with two walls. The second test was carried to obtain the flow characteristics in the atrium changing the fire source location (center, in and near corner) and ratio of inlet-outlet opening areas.

### 2. Experimental Procedure

A model corner was made by ceramic boards configuring 1.7m x 1.7m x 3m(H) with a floor of 1.0m x 1.0m. A flat diffusion gas burner, 0.1m x 0.1m with 0.03m thick, was set in and near corner changing the distance to the walls. Setting positions employed are  $S/D=0, 0.5, 1.4, 2.0, 2.8, 4.0, 5.7$  and 8.0 with using 1.5kW, 4.5kW, 7.5kW and

15kW fire. The square burner has two distances,  $S_1$  and  $S_2$ , between each facing wall. The representative distance,  $S$ , between the burner and walls was adopted as  $S = \sqrt{S_1 \cdot S_2}$ . In the case of the one side of the burner touches to the wall,  $S_1=0$ , the other distance,  $S_2$ , was adopted as the representative distance  $S$ .

Thermocouples and bidirectional were set on a rake with 5cm - 10cm (in far region from a main trajectory) separation, and the rake was moved from 0.2m to 2.4m with 20 - 60cm (in far region from a fire source) separation.

Flame tip height was evaluated based on the visual records by a video system. A 300 successive frames, 10 sec time length, were adopted to evaluate the average flame height and its deviation.

The reduced scale model of 1.8m x 1.8m x 4.5m (H) was used. Inlet openings, 10cm - 90cm with 15cm(H), were set at the center of every side taking lower inlet opening area of 0.0, 0.03, 0.06, 0.18, and 0.54m<sup>2</sup>. Outlet openings of 10cm x 15cm(H) were set underneath the ceiling of every sides and. The same gas burner as used in the first test was also used setting at the center ( $S/D=9.0$ ), and  $S/D=0$ , and 0.5. Flame height, temperature, upward velocity, air velocity at inlet openings, and differential pressure between the reduced model and environment were measured.

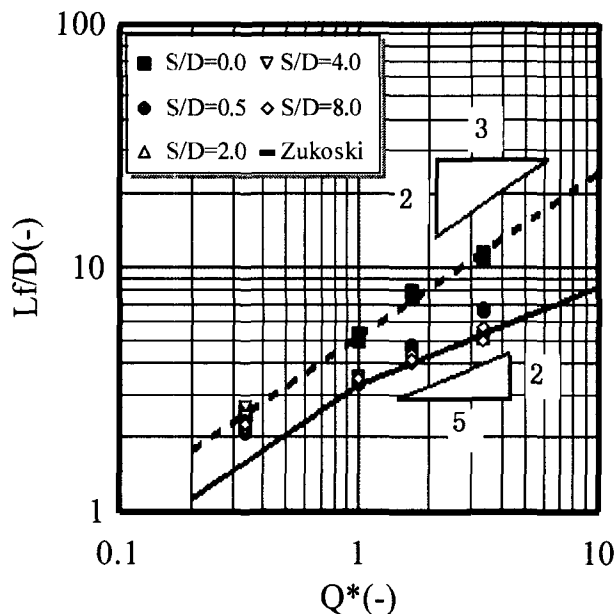


Figure 1 Normalized flame height as function of dimensionless heat release rate in and near corner fire. Rigid line was estimated by Zukoski model [4].

modification on chemical reaction into the Sugawa's model. Remembering McCaffrey's [6] report and assuming the width of the plume extend with n-th power of height,  $Z^n$ , we could present the dimensionless flame height,  $L_f/D$ , as function of dimensionless heat release rate as,

### 3. Results and Discussion

#### a) Flame Height

Figure 1 shows the relation between the dimensionless flame height,  $L_f/D$ , and dimensionless heat release rate,  $Q^*$ , when a fire source moved along the 45deg line ( $S_1:S_2=1:1$ ). This figure clearly shows that the flame height behavior has at least two modes; in the case of  $S/D \geq 2$ , flame height can be simulated by Zukoski model [4]. However, when  $Q^*$  reduced lower than 1 and the fire source moved closer to the wall as  $S/D \leq 0.5$ , flame height showed higher than the model [4]. The flame extension behavior was reported by Sugawa et al. [5] taking multi fire sources. Their model dealt with no explicit air entrainment into flames. Figure 1 and observation suggested clearly apparently that the walls gave some limitation on air entrainment into a flame and which needed some modification

$$(L_f/D) = \alpha \cdot Q^{* \frac{2}{2n+1}} \quad (1)$$

Flame from a corner or near corner fire extended with increase of  $Q^{*2/3}$ , as shown in Figure 1. From the corner test results, we obtained  $n=2$  and  $\alpha=3.3$  for an open space fire, and  $n=1$  and  $\alpha=5.3$  for a corner fire, respectively. This implies that corner flame shows similar behavior as was observed from a line fire but the constant of  $\alpha=5.3$  is greater than that for a line fire having of  $\alpha=4.2$  [5]. The flame extension behavior in dimensionless form for in and near corner fire is presented by  $L/L_0$  taking  $L_0$  as reference flame length given by corner fire and finally we obtain equation (2) for in and near corner fire, taking  $a=4$  and  $\beta=5.0$ .

$$\frac{L}{L_0} = \frac{3\beta(S/D)+5}{15\beta(S/D)+5} \cdot Q^{* \left( \frac{4a(S/D)}{15a(S/D)+9} \right)} \quad (2)$$

When the fire source attached to a wall, flame length can be simulated as a function of  $Q^{*2/3}$ , so that dimensionless flame height attaching to a wall and moves along the wall can be presented as

$$\frac{L}{L_0} = \frac{3\gamma(S/D)+5}{5\gamma(S/D)+5} \quad (3)$$

Figure 2 shows the representative relation between dimensionless flame height,  $L_f/L_0$ , with  $L_0=5.3Q^{*2/3}$  and dimensionless separation distance,  $S/D$ , as a fire source moves along the lines of  $S_1:S_2=1:1$  and  $1:2$  (45deg and 60deg in the corner). In the case the fire source moves with touching to wall, the similar flame extension behavior was observed and is simulated well by equation (3) taking  $\gamma=2.1$  based on the experimental results. The comparisons of the measured average flame heights with the predicted one considering the separation between corner-walls and a fire source showed that the equations (2) and (3) can be used for the prediction on flame extension behavior in and near corner fire.

The same model was applied for the estimation on flame length from fire set in and near corner in the atrium space. Figure 3 shows the observed data and simulated one by equation (2) and (3). These equations gave good coincidence with measured data so that these model are acceptable for the fire safety assessment. Wall effect on flame extension extended to about twice of

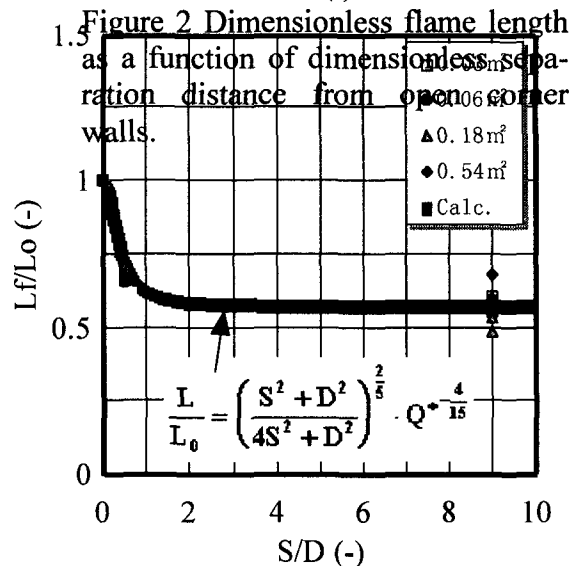
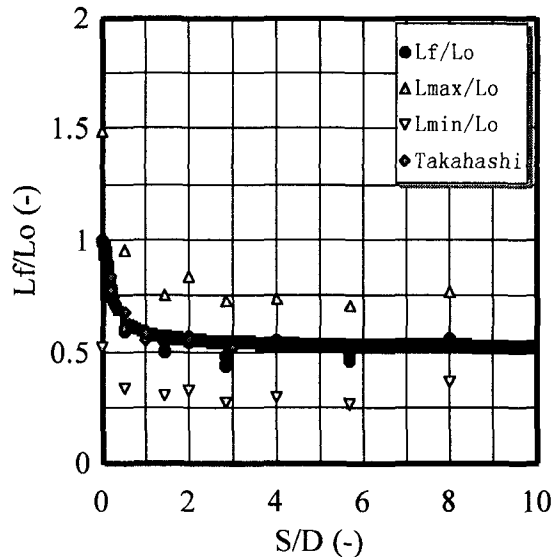


Figure 3 Dimensionless flame length as a function of dimensionless separation  $S/D$  in an atrium corner.

fire source size,  $S/D=2$ , with and without enclosure.

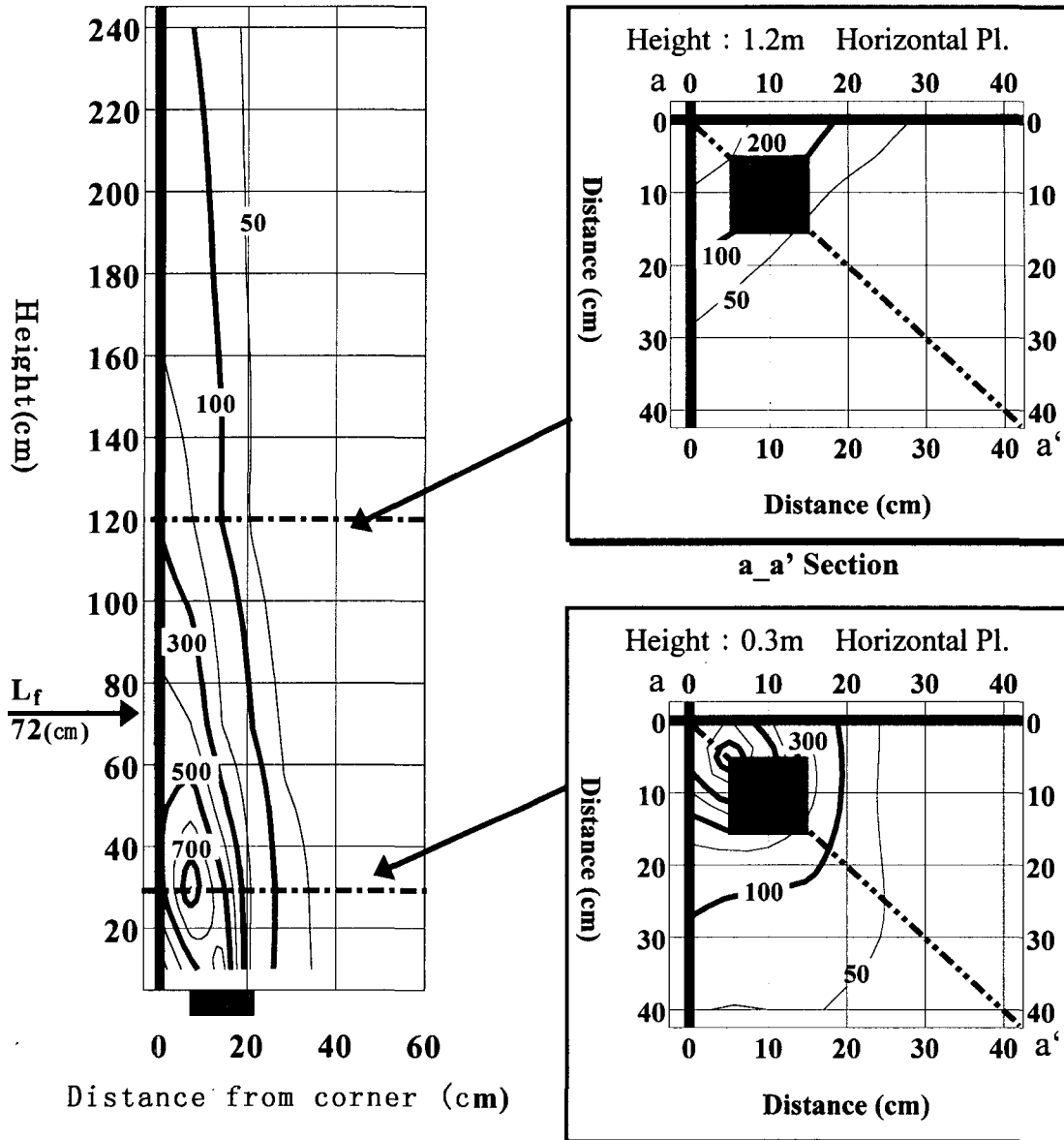


Figure 4 Representative contour maps of the excess temperature obtained for near corner fire. Vertical and horizontal contour maps and average flame height,  $L_f$ , are also illustrated. 15kW fire source was used.

b) Mass Flux along the trajectory

In order to make clear the flow behavior and mass flux of the hot current along the corner, temperatures and upward velocities were measured systematically. Figures 4 shows the representative temperature contour maps as the fire source set near corner. Mass flux of the upward current was estimated numerically based on the experimental data of upward velocity and density (based on temperature) as  $\dot{m}_p \approx \int \rho \cdot v \cdot dA$ . To carry out the integration numerically, within the 85% region (or N=15%) of temperature (or density) and upward velocity values at the main trajectory were adopted as flow region based on the contour maps of Figure 4.

Figure 5 shows the representative relation between  $\dot{m}/Q^{1/3}$  and height. Applying the point source model and considering the corner effects (plume cross section is forced to reduced to 1/4 roughly, and assuming no wall friction effect), upward mass flux can be estimated as ;

$$\dot{m} = 0.833 \kappa \rho_{\infty} \sqrt{g} (z + 1.5 \sqrt{A_f})^{5/2} \cdot Q^{1/3} \dots \dots \dots (4)$$

Figure 5 shows the mass fluxes taking fire source locations of S/D=0, 0.5 and 2 with respective the correction factor of  $\kappa = 0.33, 0.43, \text{ and } 1.0$ , which were experimentally defined. These show definitely that the corner walls gave limitation of air entrainment into flame/plume resulting small increasing of upward mass flux for in and near corner fire.

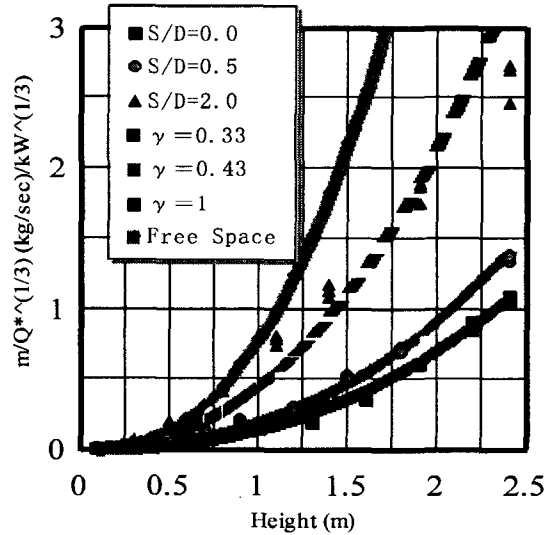


Figure 5 Mass flux normalized by  $Q^{1/3}$  as a function of height along the trajectory for in and near corner fire.

Table 1 Mass Flux (kg/sec) in the Atrium Space Model

Q kW	Location	Inlet Opening Area (m <sup>2</sup> )	Measuring Height (m)						
			0.1m	0.5m	1.0m	1.5m	2.0m	3.0m	4.0m
1.5	S/D=0.0 (Center)	0.06m <sup>2</sup>	0.019	0.095	0.261	--	0.563	0.427	0.562
4.5	S/D=0.0 (Center)	Closed	0.014	0.052	0.239	--	0.530	0.674	0.720
		0.06 m <sup>2</sup>	0.028	0.208	0.272	--	0.681	0.620	0.680
		0.18 m <sup>2</sup>	0.031	0.128	0.293	--	0.752	0.520	0.647
		0.54 m <sup>2</sup>	0.009	0.062	0.172	--	0.548	0.566	0.753
	S/D=0.5	0.06 m <sup>2</sup>	0.010	0.027	0.044	0.087	0.202	0.303	0.285
		0.54 m <sup>2</sup>	0.012	0.027	0.050	0.081	0.205	0.380	0.237
	S/D=0.0	0.06 m <sup>2</sup>	0.006	0.015	0.030	0.066	0.173	0.286	0.216
		0.54 m <sup>2</sup>	0.005	0.013	0.031	0.064	0.174	0.333	0.237
7.5	S/D=0.0 (Center)	0.06 m <sup>2</sup>	0.039	0.232	0.352	--	0.770	0.750	0.785

Wall effects on flame length within the range of  $S/D \leq 2$  and this range is almost equal to the range where the multi fire sources interact with each other as Sugawa reported [5].

The same numerical procedure,  $N=15\%$ , was adopted to evaluate the mass flux in the atrium space and the results are tabled in Table 1.

As shown in Figure 6 and 7, the active entrainment was observed above the height of  $Z/Q^{2/5}=0.8$  when periphery of the plume touched to the inner walls of the atrium and which related to the height of smoke layer. For a corner and near corner fire, equation (4) is also used to estimate the mass flux along the corner as shown in Figure 6. This equation gave good coincidence with the data in lower part of the flame region. However, for higher plume region, this gave poor simulated evaluation.

In order to make clear the neutral height in the atrium which correlate to the depth of smoke layer as a function of the fire source location, pressure difference between inside and outside of the atrium were measured. The corner and near corner fire gave double gradients in pressure distribution for vertical direction, as shown in Figure 8. The solid line in the figure means the middle height of the atrium model. The neutral height decreased with increase of  $k=(\text{inlet-area})/(\text{outlet-area})$  ratio. This figure implies that the corner fire gave highest neutral height and centered fire gave lowest neutral height. The corner walls blocked air entrainment into the flame resulting the smallest increment of plume mass flux and highest smoke layer temperature. These gave the highest neutral height for the corner

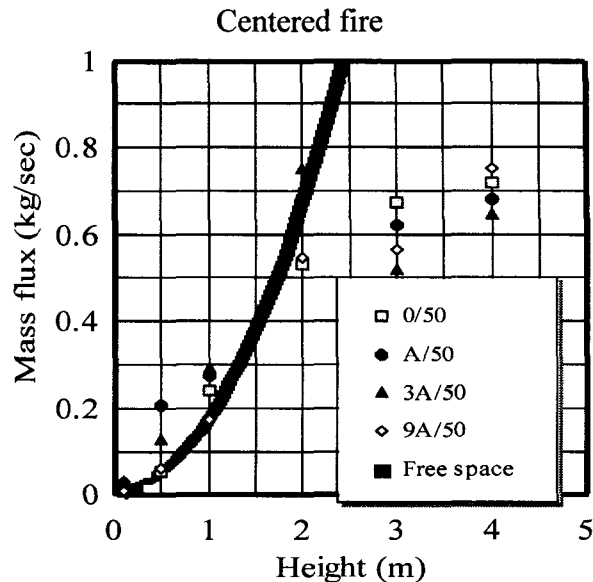


Figure 6 Mass flux in atrium as a function of height in the case of centered fire. The symbol "A" means floor area.

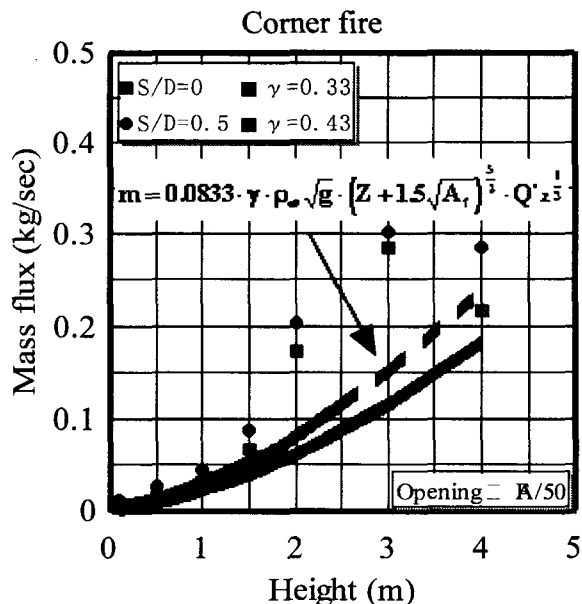


Figure 7 Mass flux along the trajectory in the atrium model in case of the fire located in and near corner, with inlet opening area of  $A/50$ .

fire than those from the centered and near corner fires.

c) Excess Temperature and Velocity Distribution for vertical direction

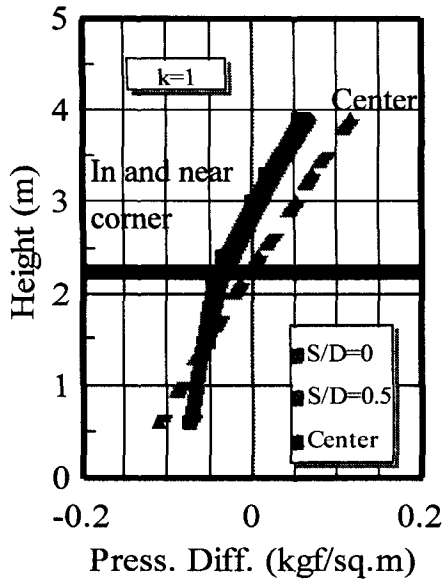


Figure 8 Pressure difference between inside and outside of the atrium changing the fire source location.

changing the fire source locations. Decreasing modes are divided into three regions and which are similar to those observed for an open fire. In case of the fire source set in corner, however, changing points of the decreasing modes were shifted upper. Corner walls blocked the air entrainment into the flame when the fire source was set in and near corner so that flame extended to higher location giving extended higher temperature than that of open fire. Door jets from inlet openings attacked directly to the base part of flame resulting lower temperature in flame region than that of open fire. As fire source was set near corner and not in corner, air entrainment into flame is partly blocked in the lower part of plume region and which resulted the middle decreasing modes between those of open fire and corner fire as shown in

Decreasing modes of the excess temperature and upward velocity distribution for vertical direction are apparent index to understand flow behavior comparing those obtained for open fire. Figure 9 shows the excess temperature distribution along the trajectory with

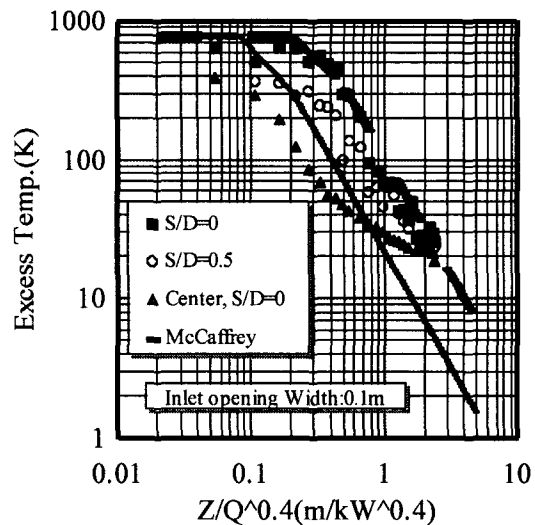


Figure 9 Excess temperature distribution along the trajectory in atrium.

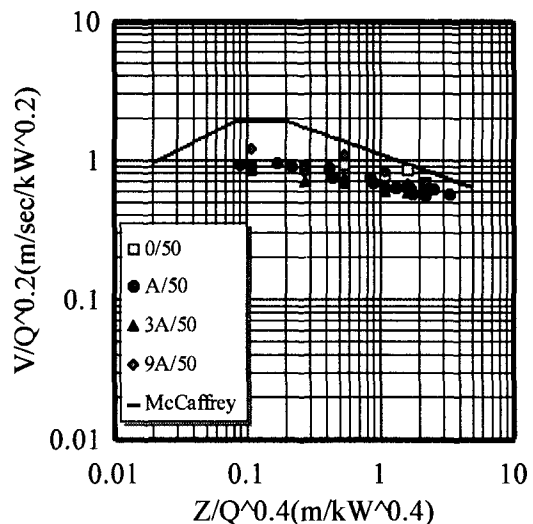


Figure 10 Upward velocity distribution along the trajectory effected with walls in open and atrium space. Fire source was set at the center.

Figure 9. The same manner were also observed in the decreasing modes of upward velocity as shown in Figure 10.

#### 4. Summary

When a fire was set in or near corner of the tall and narrow atrium, corner walls blocked air entrainment into a flame. This blocking gave flame leaning toward the corner and extension in flame length. This small air entrainment gave hotter and shallow smoke layer in the atrium space than that from centered fire and resulted in the slower smoke filling rate than that from the centered fire. This phenomena suggests that the most sensitive fire location on the fire safety assessment for the tall and narrow atrium space is the centered fire.

The flame extension behavior in and near corner was modeled by simplified equation, and it is useful to estimate the flame length in and near corner even in the atrium space.

#### 5. Acknowledgment

We would like to sincere thanks to Mr. T. Kawasaki, Ms. M. Kihara, and Ms. C. Yoneyama (under graduate students of Science University of Tokyo) for their supports in carrying out of the experiments.

#### 6. References

- 1) J. H. Klote and A. A. Milke "Design of Smoke Management System" ASHRE 1992, pp.107-108
- 2) H. Satoh, O. Sugawa, and Y. Oka, "Flame Height from Rectangular Fire Sources Considering Mixing Factor", Proc. 3rd Inter. Symp. On Fire Safety Science, IAFSS, pp.435-444 (1991)
- 3) H. Satoh, O. Sugawa, and H. Kurioka, "Modeling on Temperature and Ventilation for Fire in a Tall and Narrow Atrium", J. AIJ No. 463, pp.1-10 (1997)
- 4) E. E. Zukoski, T. Kubota, and B. Cetegen "", Fire Safety Journal, No.3, pp107-121, (1980/1981)
- 5) O. Sugawa and W. Takahashi "Flame Height Behavior from Multi Fire Sources" Fire and Materials, vol.17, No.3, pp.111-118
- 6) B. J. McCaffrey The SFPE Handbook of Fire Protection Eng., Sec.1, Chap.18, NFPA (1988)

#### 7. Nomenclature

$A_f$ : area of fire source

$C_p$ : specific heat

$D$ : representative length of fire source

$g$ : gravity acceleration

$L_f$ : flame length (flame height)

$S_1$  and  $S_2$ : separation distance from walls to fire source,

$Q^*$ : dimensionless heat release rate

$$Q^* = \dot{Q} / \rho_{\infty} C_{p_{\infty}} T_{\infty} \sqrt{g D D^2} :$$

$T$ : temperature

$\rho$ : density ,

subscript  $\infty$  : ambient

